Changes in the Spread of the Variability of the Seasonal Mean Atmospheric States Associated with ENSO

Arun Kumar

Climate Modeling Branch, EMC, NCEP/NWS/NOAA, Washington, District of Columbia

Anthony G. Barnston and Peitao Peng

Climate Prediction Center, NCEP/NWS/NOAA, Washington, District of Columbia

Martin P. Hoerling

Climate Diagnostics Center, NOAA/CIRES, Boulder, Colorado

Lisa Goddard

Experimental Forecast Division, IRI/SIO, La Jolla, California

(Manuscript received 14 June 1999, in final form 28 September 1999)

ABSTRACT

For a fixed sea surface temperature (SST) forcing, the variability of the observed seasonal mean atmospheric states in the extratropical latitudes can be characterized in terms of probability distribution functions (PDFs). Predictability of the seasonal mean anomalies related to interannual variations in the SSTs, therefore, entails understanding the influence of SST forcing on various moments of the probability distribution that characterize the variability of the seasonal means. Such an understanding for changes in the first moment of the PDF for the seasonal means with SSTs is well documented. In this paper the analysis is extended to include also the impact of SST forcing on the second moment of the PDFs.

The analysis is primarily based on ensemble atmospheric general circulation model (AGCM) simulations forced with observed SSTs for the period 1950–94. To establish the robustness of the results and to ensure that they are not unduly affected by biases in a particular AGCM, the analysis is based on simulations from four different AGCMs.

The analysis of AGCM simulations indicates that over the Pacific–North American region, the impact of interannual variations in SSTs on the spread of the seasonal mean atmospheric states (i.e., the second moment of the PDFs) may be small. This is in contrast to their well-defined impact on the first moment of the PDF for the seasonal mean atmospheric state that is manifested as an anomalous wave train over this region. For seasonal predictions, the results imply that the dominant contribution to seasonal predictability comes from the impact of SSTs on the first moment of the PDF, with the impact of SSTs on the second moment of the PDFs playing a secondary role.

1. Introduction

Extratropical seasonal climate anomalies go through considerable interannual variability. This variability can be characterized in terms of probability distributions. An idealized example of this is illustrated in Fig. 1a, where the probability distribution for the variability of the seasonal means of some atmospheric variable at a particular geographical location is shown. Such probability distributions can be constructed from the analysis of seasonal mean observed data. For example, historical data of the observed 500-mb seasonal mean heights at given geographical locations can be used to approximate the probability distributions characterizing interannual variability of this quantity at those locations for a particular season. Different moments (e.g., mean, standard deviation, skew, etc.) of probability distributions define the *expected climate*.

Interannual variations in the sea surface temperature (SST) forcing can influence different moments of climatological probability distribution. An example of this is shown in Fig. 1a, where the probability distribution of some variable for an anomalous SST forcing (e.g.,

Corresponding author address: Dr. Arun Kumar, Climate Modeling Branch, EMC/NCEP, 5200 Auth Road, Rm. 807, Camp Springs, MD 20746.
E-mail: arun.kumar@noaa.gov

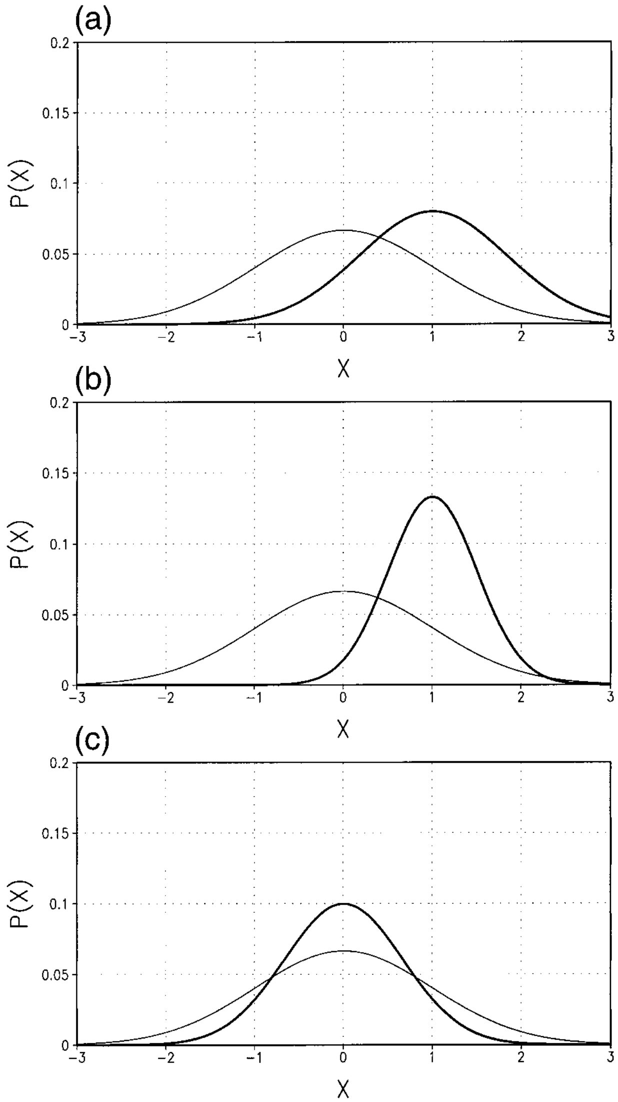

FIG. 1. A schematic for different probability distribution functions (PDFs) for the seasonal mean 500-mb heights at some geographical location. Two curves in each panel show the climatological PDF (light curve) and the PDF of seasonal mean heights for the anomalous SST state (dark curve). Three possible scenarios for the impact of SST on the seasonal mean heights are depicted. (a) The case when the impact of an anomalous SST state is primarily on the mean of the PDF. (b) The case when both mean and spread of the PDF for the seasonal means atmospheric heights are affected by the anomalous SSTs. (c) The case when only the spread of the PDF is affected by the SSTs, for example, during the years when the SSTs may be close to normal.

El Niño) together with its climatological distribution is shown. The difference between the two probability distributions characterizes the extent to which the SST forcing influences the seasonal atmospheric time mean state. It is a well-known fact that even for a fixed SST forcing the extratropical seasonal time mean state is not unique (Lau 1985; Chervin 1986; Kumar and Hoerling 1995), leading to a finite width, or nonzero spread of the probability distribution. A formal distinction between two probability distribution functions (PDFs) shown in Fig. 1a needs to be emphasized; while the climatological PDF is constructed using a collection of observed seasonal mean atmospheric states associated with a wide range of SST states, the PDF for the anomalous SST forcing is constructed from the collection of seasonal mean atmospheric states associated with a fixed anomalous SST forcing (or within a certain limited range of that SST forcing).

Atmospheric seasonal predictability related to interannual variations in the SST forcing then entails understanding the influence of SSTs on various moments of the PDFs. These impacts, in general, have geographical variations and also depend on the season and on the atmospheric variable under consideration. Such impacts of interannual variations in the tropical Pacific SST forcing on the first moment of the PDF for the extratropical seasonal mean atmospheric state have been extensively analyzed and documented. For boreal winter these impacts primarily occur over the Pacific–North American (PNA) region (Horel and Wallace 1981; Trenberth et al. 1998). This understanding of the changes in the mean state in response to the remote SST forcing forms the underpinning of the seasonal prediction efforts over this region.

Interannual variations in tropical Pacific SST forcing may also impact higher-order moments of the atmospheric PDFs and therefore can also contribute to atmospheric seasonal predictability in extratropical latitudes. One such scenario is illustrated in Figs. 1a and 1b. In Fig. 1a while the primary impact of anomalous SST forcing is on the first moment of the PDF, in Fig. 1b the change in SST forcing also has a large influence on the spread (or the second moment) of the PDF. Further, the atmospheric seasonal predictability between the two cases differ, with larger predictability in the second case due to a greater reduction in the uncertainty of the atmospheric seasonal time mean state. Within this paradigm, neutral SST states will also be associated with finite atmospheric seasonal predictability. This is illustrated in Fig. 1c, where the atmospheric PDF for a neutral SST state, without any change in its first moment, has reduced spread.

In this paper we attempt to quantify the possible impact of tropical Pacific SST variability on the spread of PDFs over the PNA region. For if systematic influences on the spread of seasonal mean quantities exist (e.g., as in Fig. 1b), these can be incorporated to enhance the utility and skill of seasonal predictions.

Our analysis is primarily based on an ensemble of atmospheric general circulation model (AGCM) simulations forced with the observed SST forcing. These simulations are for the 1950–94 period. To ensure that the analysis is not unduly affected by biases in a particular AGCM, the analysis is based on simulations from four different AGCMs. These AGCMs are described in section 2. The availability of multiple realizations of AGCM simulations forced with a constant SST forcing makes it

TABLE 1. AGCMs and number of simulations for 1950–94 period for each AGCM. The horizontal and vertical resolution of each model are given in column 3. Detailed description about the respective models can be found from the references given in column 4.

AGCMs	No. of simulations	Resolution	Reference
IRI/ECHAM3	10	T[a]40L[b]18	Roeckner et al. (1992)
NCAR/CCM3	12	T42L18	Kiehl et al. (1998)
GFDL	12	R[c]30L18	Lau (1997)
NCEP/MRF9	13	T40L18	Kumar et al. (1996)

[a] Spectral triangular truncation.
[b] Number of levels in vertical.
[c] Spectral rhomboidal truncation.

feasible for us to estimate the spread of PDFs for different SST states. As described in section 2, the dependence of the spread of the seasonal means on the tropical SST forcing is next studied and is compared with the corresponding dependence of the first moment of the PDF itself. We next attempt to quantify the relative contributions of the first and second moment with respect to seasonal predictability. As described in section 2, following a procedure for the practical application to seasonal prediction, this assessment is based on categorical forecasts. Results, discussion, and conclusions, respectively, are presented in sections 3 and 4.

2. AGCMs and analysis procedure

a. AGCMs and data

Our analysis focuses on the interannual variability of 500-mb heights over the PNA region during boreal winter. Over this geographical region and for this season the remote influence of tropical Pacific SSTs on the interannual variability is known to be largest relative to its influence on other extratropical regions. The analysis is done for the January–February–March (JFM) seasonal mean and covers the 1950–94 period. The 500-mb heights for this period are obtained from the National Centers for Environmental Prediction–National Center for Atmospheric Research (NCEP–NCAR) reanalysis (Kalnay et al. 1996). In addition, the observed SSTs for the same period are obtained from the combination of two different analyses: monthly mean analyses for the 1950–81 period use in situ observations with eigenvector reconstruction to obtain global SST analyses (Smith et al. 1996). After 1981, in situ measurements together with satellite observations are sufficient to resolve the global SST field and the analysis follows an optimal interpolation procedure as described in Reynolds and Smith (1994).

All AGCM simulations are forced by observed SST variability for the 1950–94 period, and model data from four different AGCM simulations are used. For each AGCM an ensemble with a minimum of 10 model simulations were available (see Table 1). Different simulations within an ensemble for each AGCM start from different atmospheric initial states but experience identical SST forcing throughout the integration period. With the exception of Geophysical Fluid Dynamics Laboratory (GFDL) simulations, all AGCM simulations are forced by the observed global SSTs. For the GFDL AGCM, 12 available simulations can be further grouped in three different categories: in the first category, the AGCM simulations are forced with the observed evolution of global SSTs; in the second category, AGCM simulations are forced with the observed SSTs in the tropical Pacific Ocean alone, while the SSTs outside this region evolve through a climatological seasonal cycle; simulations in category three differ from those in category two in that the evolution of SSTs outside the tropical Pacific is predicted using an oceanic mixed layer model (Lau 1997). There are four AGCM simulations in each category, however, within the scope of the present analysis all 12 AGCM simulations are treated similarly, and possible inhomogeneities due to different SST forcings are neglected. This procedure is also justified based on the analysis by Blade (1999), who has shown that the changes in the extratropical seasonal mean variability are most sensitive to the SST variability in the topical Pacific, a feature common to AGCM simulations in all three categories.

b. Analysis of seasonal mean atmospheric variability with SSTs

An analysis of the impact of interannual variability in the tropical Pacific SSTs on the PDF of the seasonal mean atmospheric state over the PNA region is performed using the ensemble of AGCM simulations. Let $X_{i\alpha}$ denote the AGCM-simulated seasonal mean anomaly for the year α and realization i within the ensemble. The ensemble mean anomaly averaged over all realizations is defined as

$$\mu_\alpha = \frac{1}{n}\sum_{1}^{n} X_{i\alpha}, \tag{1}$$

where n is the number of realizations within the ensemble for the fixed SST forcing. Because of atmospheric noise, seasonal means for the individual realizations starting from different initial conditions differ and their departure from the ensemble mean μ_α is the measure of the spread. For a particular year (or for a fixed SST forcing) this spread is defined as

$$\sigma_\alpha^2 = \frac{1}{n}\sum_{1}^{n} (X_{i\alpha} - \mu_\alpha)^2. \tag{2}$$

The ensemble mean μ_α and the spread σ_α are the estimated values of the mean (i.e., the first moment) and the standard deviation (i.e., the second moment) of the PDF, which characterizes the variability of the seasonal mean quantity $X_{i\alpha}$ for a particular SST anomaly observed for the year α. For different geographical locations and for different SST forcings these can be estimated from the ensemble of AGCM realizations. Both of these quantities, in general, can depend on the interannual variations in the SSTs.

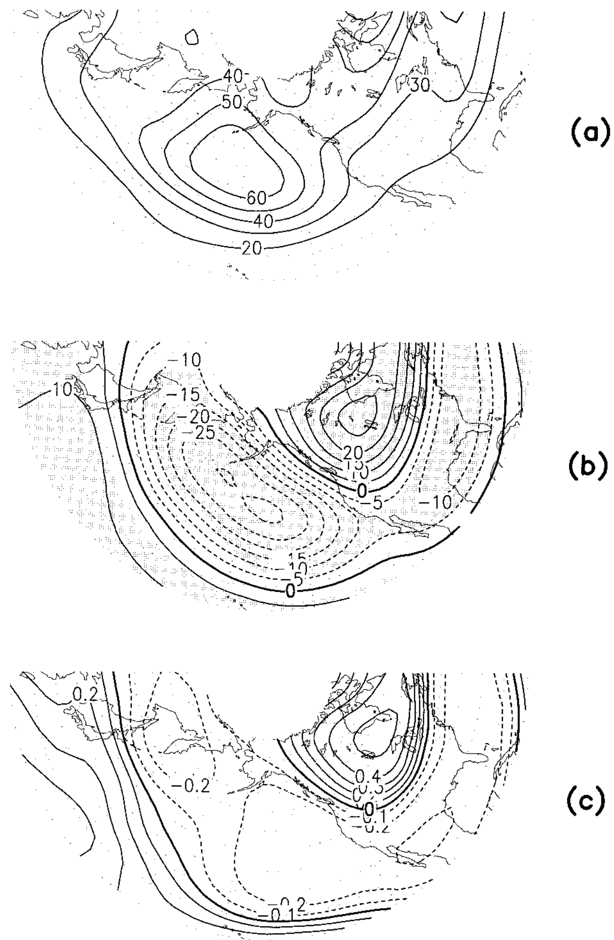

FIG. 2. (a) Standard deviation of the 500-mb seasonal mean JFM heights for observations over the PNA region. Contour interval is 20 m. (b) Linear regression between the tropical Pacific SST index and the observed JFM 500-mb heights. Anomalies are shown for the unit standard deviation of 0.83°C for the SST index. Negative anomalies are dashed, and the contour interval is 5 m. (c) Anomalous probabilities for the observed seasonal mean 500-mb heights to be in the above-normal category for a composite warm SST event in the tropical Pacific with the assumption that the spread of the PDF for the seasonal mean heights for the warm years is the same as the spread for the climatological PDF. Contour interval is 0.1 and negative anomalies are dashed. Shaded region in (b) corresponds to the spatial domain where the correlation between the SST and 500-mb height is significant at 95% confidence level (with degrees of freedom assumed to be number of years minus 2, i.e., 43).

A conventional way to estimate the impact of the interannual changes in the SST forcing on the first moment of the PDF is through linear regression maps between the ensemble mean μ_α and some suitable SST index. In a similar manner the systematic changes in the spread of the PDF due to variations in the SST forcing can be estimated by regression maps between the spread σ_α and the index for the SSTs. In our analysis of the JFM seasonal means, the SST index is taken as the area average over the spatial domain 5°S–5°N and 130°W–180°. This area is highly correlated with the El Niño–Southern Oscillation (ENSO) phenomenon and has a climatological SST value near 27° to 28°C (Barnston et al. 1997; Trenberth et al. 1998). This makes the region's SST a sensitive indicator of the remote teleconnections caused by changes in convection during ENSO episodes.

The impact of tropical Pacific SST forcing on the seasonal mean circulation variability in 500-mb heights over the PNA regions is first assessed as regression patterns between this SST index and the mean μ_α and the spread σ_α. Although the scope of such an analysis is restricted to linear relationships, the advantage of a regression approach is that it tends to minimize the sampling variations in the estimates of the mean and the spread of the PDFs due to finite ensemble sizes. Furthermore, other studies have suggested that for weak to moderate SST anomalies, the relationship between tropical Pacific SST forcing and extratropical mean climate over the PNA region may be well represented by linear dependence (Kumar et al. 1996; Kumar and Hoerling 1998; Peng et al. 2000).

c. Assessment of relative contributions to seasonal predictability

The analysis described in the previous section to assess the impact of the SST forcing on the first and the second moments of the PDF characterizing variability of the seasonal means assumes a unique PDF for each SST state. Although conceptually simple, this does, however, differ from the practical application of seasonal prediction where a single PDF is used to define the climatological variability. This climatological distribution is constructed using a collection of observed seasonal mean atmospheric states associated with a wide range of SST forcing and generally utilizes the data over some predefined ''climate normal'' period, for example, a 30-yr period from 1961 to 1990. These climatological distributions at different geographical locations are then used to define the below-normal, normal, and above-normal categories (hereinafter referred to as ABN categories) such that seasonal mean atmospheric states within the climate normal period have equal probability to be in any of the three ABN categories. In our case the climatological ABN categories at each location for observations as well for the AGCM simulations are obtained from the estimate of the spread of the respective seasonal mean atmospheric states and the assumption that the PDF of the seasonal mean atmospheric states is normally distributed. With this assumption the boundaries defining the above- and below-normal categories occur at ± 0.43 standard deviations, respectively.

Probabilistic categorical forecasts for a particular season are then made using the estimates of the PDF for the seasonal atmospheric means for that season's expected anomalous SST forcing. With the assumption of normality, estimating these PDFs entails estimates of the first and second moments obtained using a collection of seasonal mean atmospheric states for that season's anomalous SST forcing. From these PDFs, the anom-

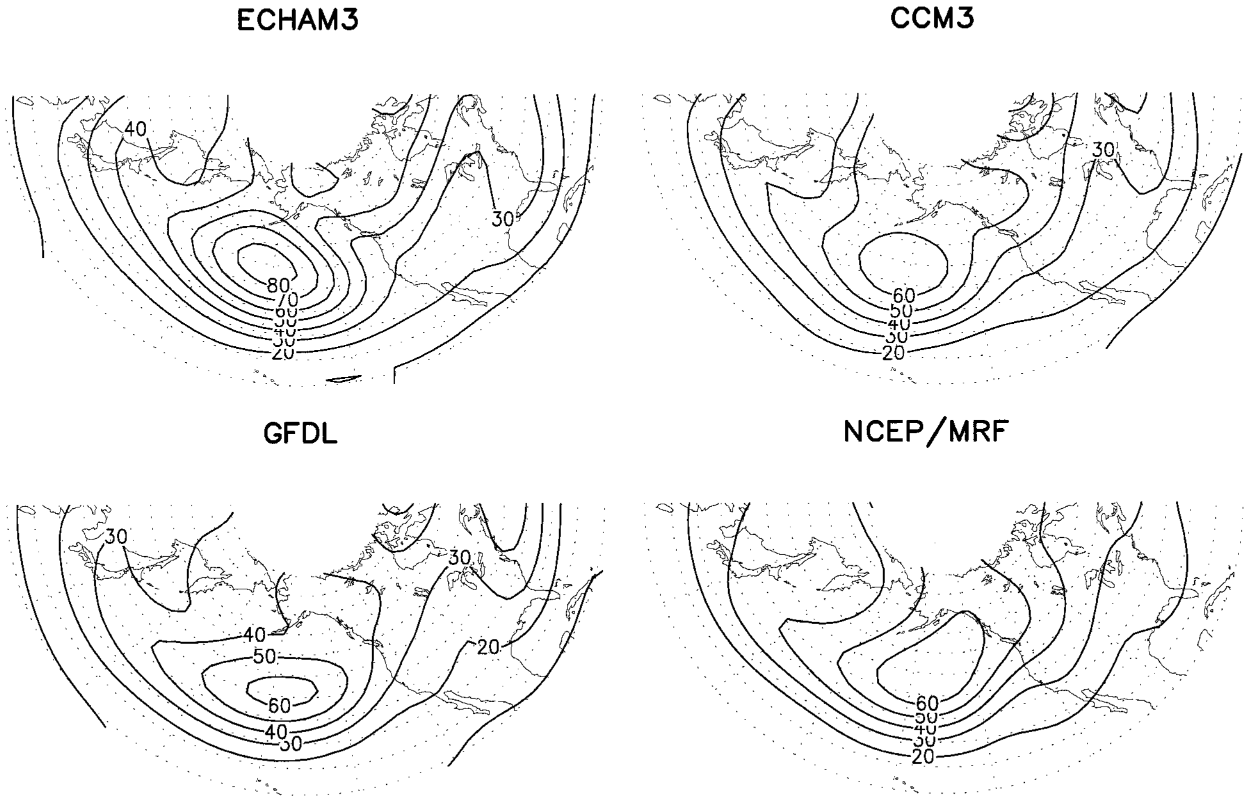

FIG. 3. Standard deviation of the 500-mb seasonal mean JFM heights simulated by four AGCMs. Contour interval is 20 m. These standard deviations can be compared with those for the observed shown in Fig. 2a.

alous probabilities for the seasonal atmospheric means to be in different ABN categories at different geographical locations are determined. Within this framework changes in the mean as well as the spread of the PDFs lead to atmospheric seasonal predictability.

The availability of an ensemble of AGCM simulations allows us to estimate the first and the second moments of the PDF associated with seasonal atmospheric means for that year's SST forcing. Although this procedure can be followed for each JFM, for brevity and for the fact that the ensemble size for individual AGCMs is not large enough to reliably estimate the spread for individual SST states, the analysis is done after defining a composite warm and cold tropical Pacific SST event. Following this, three sets of probability distributions are constructed: 1) PDFs for the climatological distributions for the seasonal mean 500-mb heights utilize the AGCM simulations for all 45 yr, 2) PDFs for the ''warm SST years'' utilize the AGCM simulations only for those JFMs when the tropical Pacific SST index is above one standard deviation, and 3) PDFs for the ''cold SST years'' utilize the AGCM simulations for the JFMs when the tropical Pacific SST index is more than one standard deviation below the mean. We also assume that PDFs of the seasonal mean 500-mb heights are normally distributed, and therefore, the mean and standard deviations are sufficient to completely specify the PDF. The validity of this assumption is discussed by Zwiers (1996) and Rowell (1998). The seasonal mean 500-mb height anomalies for each season are computed relative to their 1950–94 ''climatology'' for the respective AGCM.

The relative impact of SST on the mean and spread of PDF is next assessed by comparing the anomalous probabilities for ABN categories due to changes in the mean with and without including the changes in the spread of the PDF. In other words, categorical probabilities are first obtained with changes in the mean of the PDF alone and by assuming that the spread of the PDF for anomalous SST states remains equal to its climatological value. These are then compared with the categorical probabilities when the impact of the anomalous SST state on the mean as well as on the spread are included. The difference between the two gives a relative measure of the impact of SSTs on the atmospheric seasonal predictability from changes in the spread of the seasonal mean atmospheric states.

3. Results

a. Analysis of interannual variability in the mean and the spread

Before the analysis of the interannual variability of 500-mb heights and their relationship to the tropical

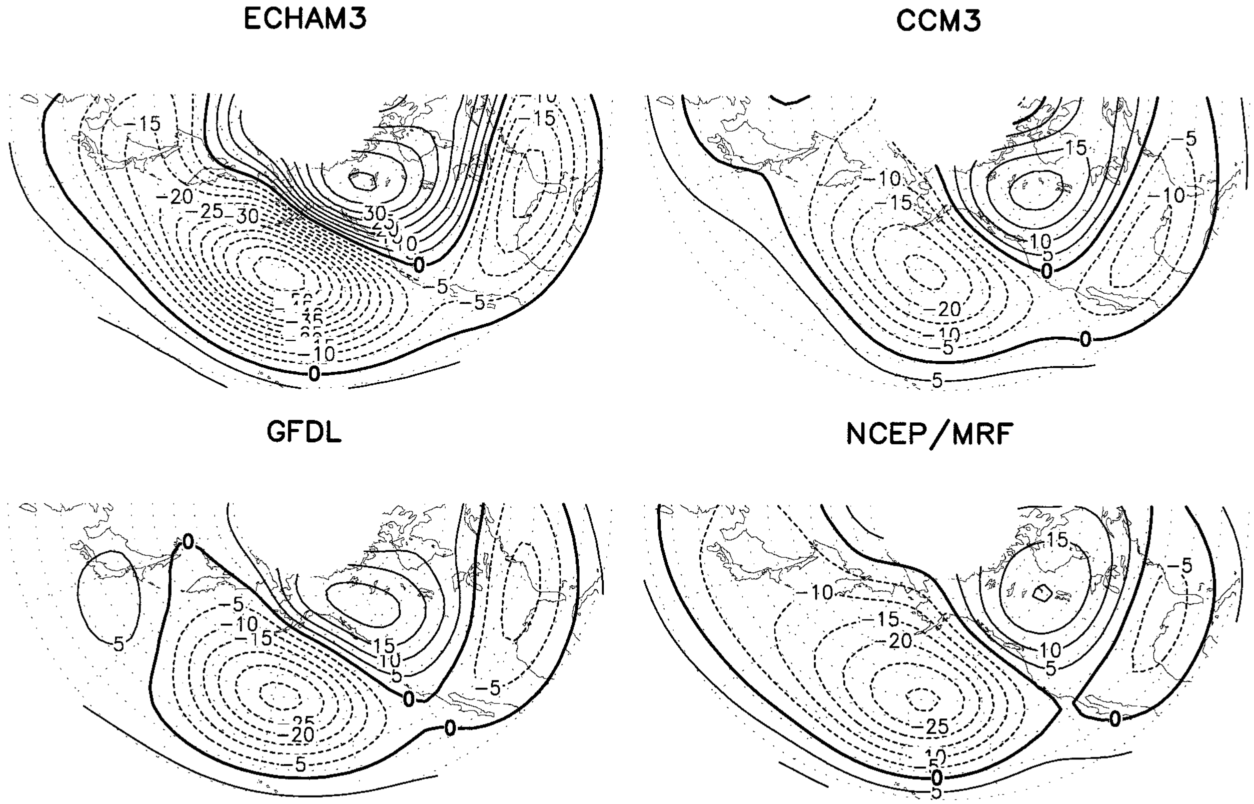

FIG. 4. Linear regression between the tropical Pacific SST index and AGCM simulated 500-mb seasonal mean JFM heights. Heights are shown for the unit standard deviation of 0.83°C for the SST index, and the regressions were performed between the ensemble-averaged heights (i.e., the estimate for the mean of the PDF) and the SST index. Negative anomalies are dashed and contour interval is 5 m. Because of larger sample size, the spatial domain over which the SST–height correlation is statistically significant at 95% confidence level spans almost the entire domain and, for the sake of clarity, is not shaded.

Pacific SST forcing, the total variability of JFM means for the four AGCMs is first compared with observations. The observed standard deviation of 500-mb JFM heights for the period 1950–94 over the PNA region is shown in Fig. 2a. This can be compared with the corresponding variability in four different AGCMs shown in Fig. 3. For the AGCMs, the standard deviations are first obtained for each AGCM simulation for the 1950–94 period and then are averaged over all such simulations within the ensemble.

The spatial pattern of interannual variability for all four different AGCMs, in general, has good spatial correspondence with observations, with the maximum in variability located to the south of Alaska. The maximum amplitude of seasonal variability in the ECHAM3 AGCM is somewhat larger than its observational counterpart. This comparison for the interannual variability of 500-mb JFM seasonal heights between AGCMs, and the observations ensure that at least for this field the AGCMs are not unduly biased and possess interannual variability comparable to that in the observations.

We next proceed to analyze the impact of the interannual changes in the tropical Pacific SST forcing on the mean and the spread of the PDFs. As discussed before, the SST variability is characterized in terms of an area-averaged SST index. Because for a given SST forcing only a single observed realization is available, estimates of geographical distribution of the spread for the 500-mb seasonal mean JFM heights for a fixed SST forcing are not feasible. The variations in the mean of the PDF, that is, μ_α with the SST variability, however, can be estimated. In particular, the linear component of the dependence of μ_α on the SSTs is estimated by linear regression between the observed 500-mb heights and the tropical Pacific SST index. This regression map is shown in Fig. 2b and is reminiscent of the familiar atmospheric response to tropical Pacific SST anomalies (Horel and Wallace 1981; Kumar and Hoerling 1997).

At each geographical location, the component of the shift in the PDF for the 500-mb seasonal height, which is linearly related to the interannual changes in the SST index, is characterized by the magnitude of the regression in Fig. 2b. Larger regressions imply larger shifts in the PDF, while the PDF at the geographical locations close to the zero lines have no impact on their means.

Corresponding regression maps for four different AGCMs are shown in Fig. 4. These regression maps are obtained by linearly regressing the ensemble mean sig-

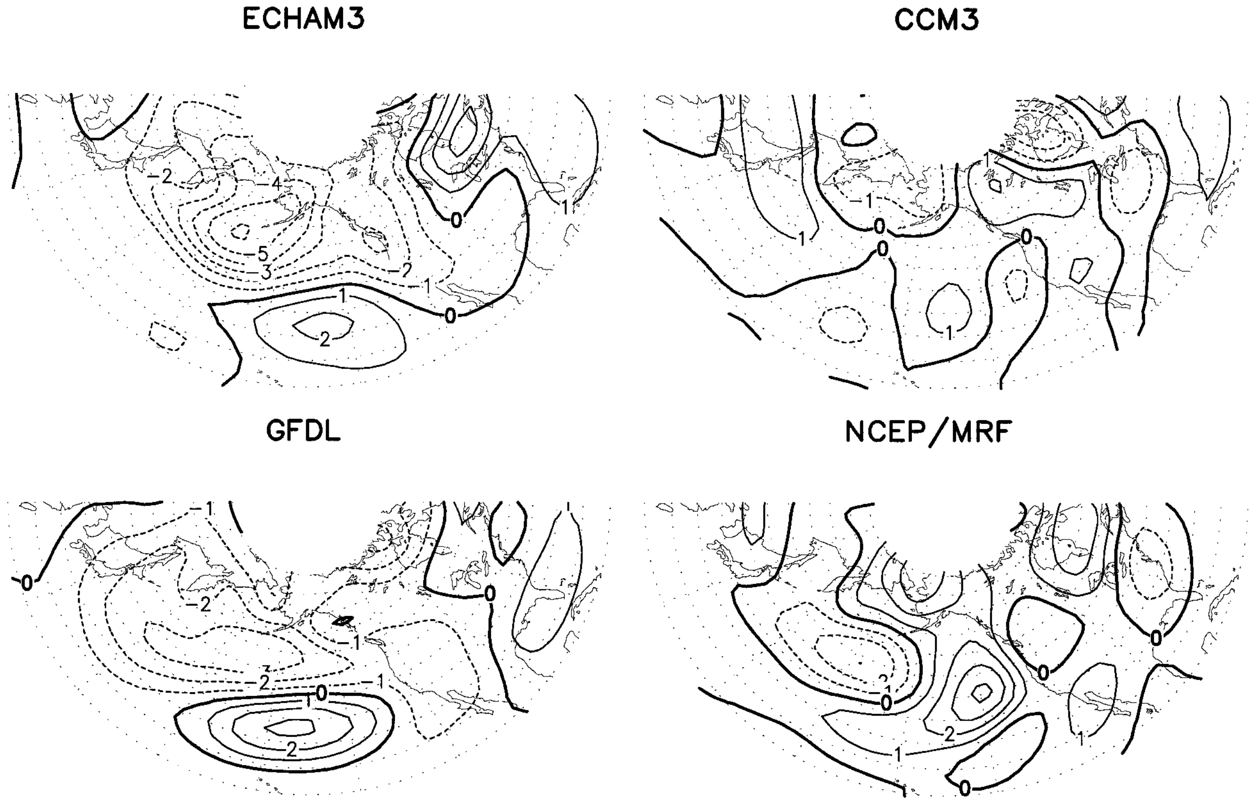

FIG. 5. Linear regression between the tropical Pacific SST index and the AGCM simulated spread for the 500-mb seasonally averaged JFM heights. Change in the spread is shown for the unit standard deviation of 0.83°C for the SST index. Negative anomalies are dashed, and contour interval is 1 m.

nal μ_α in Eq. (1) upon the SST index. We should point out that regressions so obtained are equivalent to the average of regressions obtained from individual AGCM simulations when the averaging is performed over *n* simulations within the ensemble. The spatial pattern of the regression for all four AGCMs is very similar to that in the observations (Fig. 2b). The implied shift in the mean of the PDF of 500-mb JFM heights is largest for the ECHAM3. For the other three AGCMs the magnitude of the linear signal in the mean of the PDF is quite comparable to that in the observations.

Linear regression maps for the interannual variations in the spread of the PDF [i.e., Eq. (2)] with SST index are shown in Fig. 5. We should point out that linear regression has a limitation in its applications to the spread because the spread does not have a Gaussian distribution even though the 500-mb height itself does. The distribution of the spread is positively skewed; however, this characteristic becomes less severe as the ensemble size increases. For the ensemble size of 10 or 12 used here the skewness is noticeable but not overwhelming, and the regression approach gives an acceptable first-order approximation to the strength of the SST–spread relationship. Unlike the changes in the mean of the PDF shown in Fig. 4, the linear impact of SSTs on the changes in the spread of the PDF among four different AGCMs shares less commonality and has smaller spatial scales. A feature that appears to be common among the AGCMs is that the spread of the seasonal mean heights south of Alaska tends to be reduced for positive SST anomalies.

The relative magnitude of the influence of changes in the SST on the mean and spread of the PDF of 500-mb height anomalies can be assessed by comparing Figs. 4 and 5. In general, the impact of SSTs on the mean of the PDF of 500-mb JFM heights is more systematic and dominates over their impact on the spread. Similar conclusions from the analysis of the interannual variability of spread, area averaged over the PNA region, were also reported by Kumar and Hoerling (1998). Zwiers et al. (2000) also find only a weak influence of different SST states on the internal variability of the seasonal mean atmospheric states. The relative impact of the two on the seasonal predictability is further quantified later in this section.

To ensure that the regressions shown in Fig. 5 are not unduly affected by the linearity inherent in the analysis, we have further analyzed the changes in the spread with SSTs based on composites. A similar analysis for changes in the mean have already been discussed by Hoerling et al. (1997) where evidence for nonlinearity of the change in the mean state for the warm versus cold SST

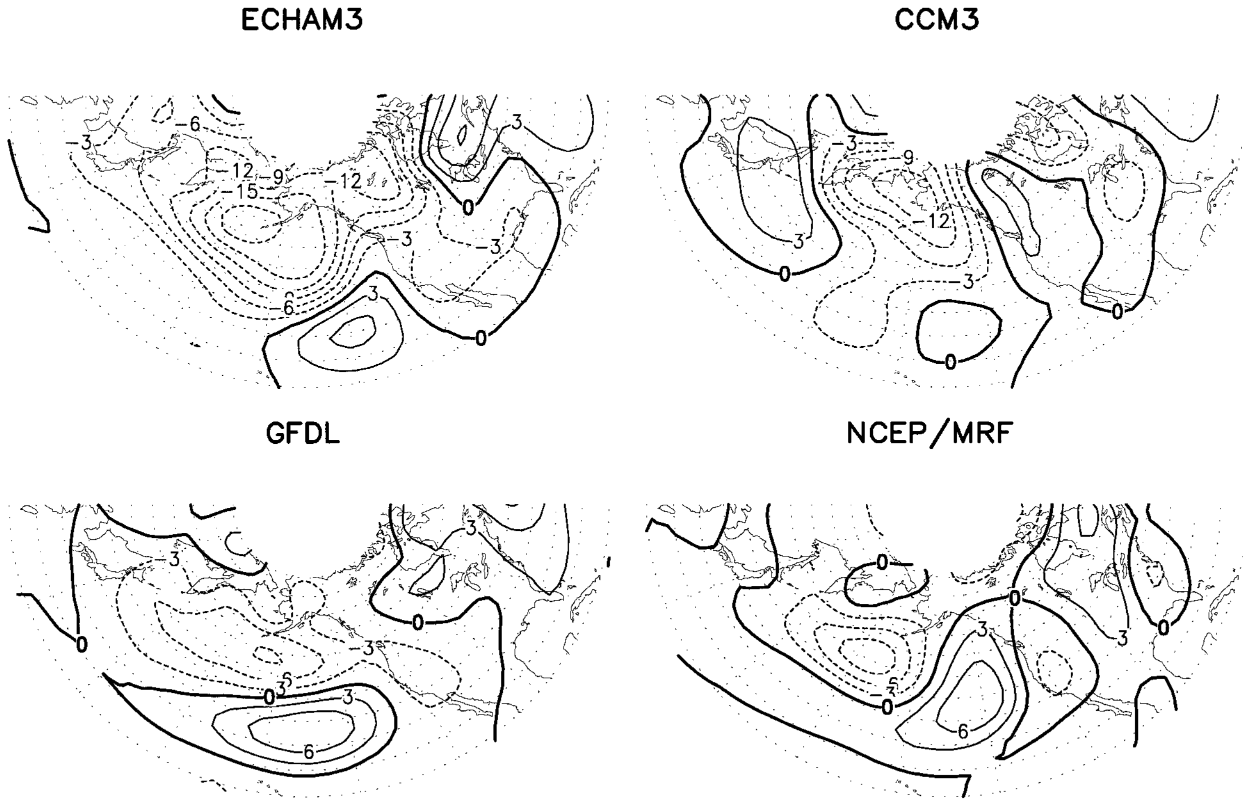

FIG. 6. Difference in the standard deviation (or spread) of the 500-mb heights between composite warm and neutral SST years as simulated by four AGCMs. The warm (cold) SST events in the period 1950–94 are defined as those when the anomalous SST index is at least one standard deviation above (below) normal. All the other years are defined as neutral years. Negative anomalies are dashed and contour interval is 5 m.

events was presented. To compare the composites for the spread during warm and cold SST events with the spread during the normal years, the warm and cold SST events in the period 1950–94 are defined as those when the anomalous SST index is at least one standard deviation above or below normal. All the other years are defined as normal years.

The difference in the mean spread for warm and cold SST years relative to the normal years is shown in Figs. 6 and 7, respectively. Similar plots for the mean composite anomalies for warm and cold events complementing the regression maps in Fig. 4 can also be made. These, apart from differences in magnitude, are similar to regression maps shown in Fig. 4 and are not reproduced here. It is immediately apparent that the impact of warmer tropical SST states on the spread of the seasonal means over the PNA region is larger and more systematic than for the cold SST events. The impact of SSTs on the spread, therefore, may be nonlinear between warm and cold events. This nonlinearity between the spatial pattern for the changes in spread between warm and cold events may be larger than that corresponding for the mean shift where the warm and cold composite seasonal mean anomalies tend to have more similarity in their spatial structure (but with opposite phase; Hoerling et al. 1997).

During warm events and for all four AGCMs, the spread tends to be suppressed in the North Pacific. However, a systematic and opposite increase in the spread for cold SST events is not found. This nonlinearity between the warm and cold events is possibly the cause for the weak linear signal in the spread with SSTs shown in Fig. 5. Statistical significance of the spatial patterns in Figs. 6 and 7 is discussed in the appendix.

As was discussed earlier, changes in both mean and the spread of the PDF as a function of the tropical Pacific SST state can contribute to seasonal atmospheric predictability. For example, the regions with reduced spread in Fig. 6 imply increased predictability for the seasonal means. To quantify their relative contribution, the approach of categorical probabilistic seasonal forecast is followed. Results are only shown for the composite warm SST events since for the cold SSTs the impact of SST on the spread is small (Fig. 7).

b. Assessment of relative contributions of changes in the mean and spread to seasonal predictability

Assuming that 500-mb heights are normally distributed and using the procedure described in section 2c, for each AGCM and at each geographical location, ABN categories based on the estimate of the climatological

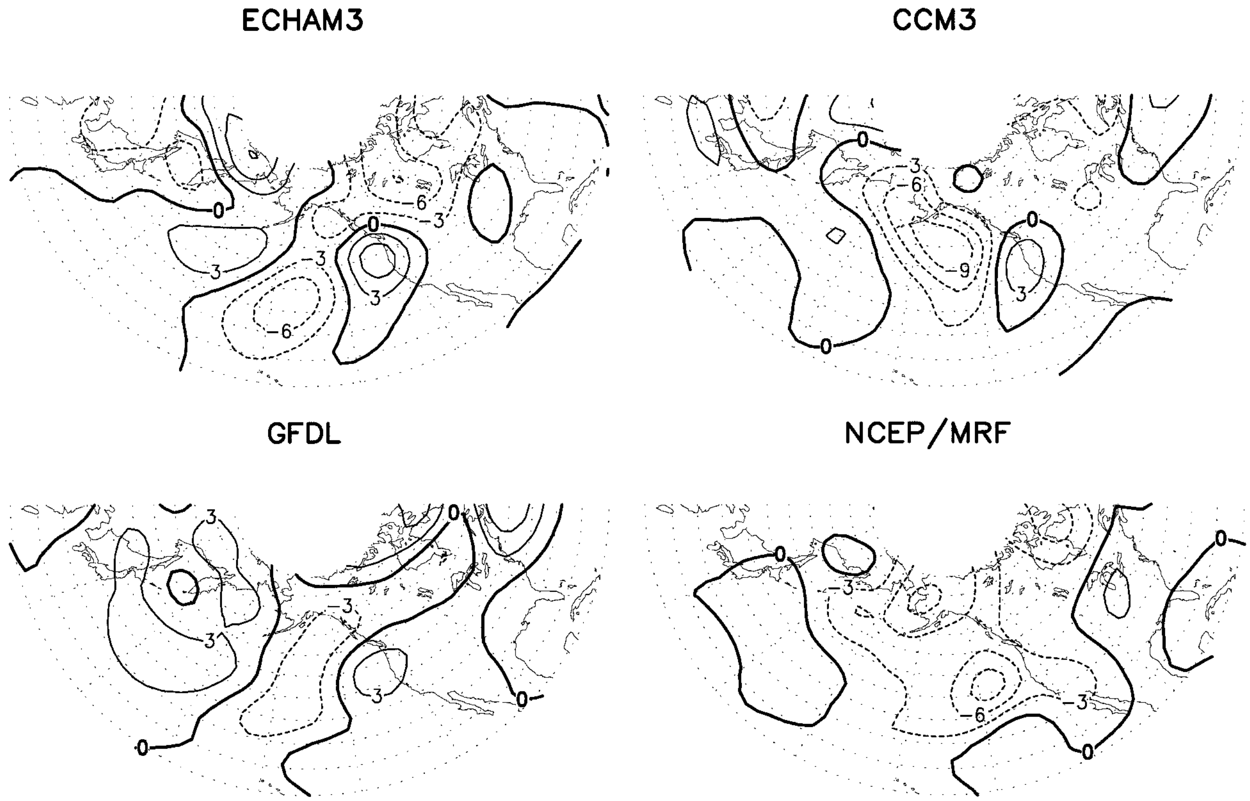

FIG. 7. Same as for Fig. 6 but for the difference in spread between the composite cold and neutral SST years.

spread shown in Fig. 3 are first estimated. For the composite warm event we next estimate the anomalous probabilities for the seasonal means to be in the below-normal, normal, or above-normal categories. This entails first estimating the seasonal mean height anomaly and the spread of seasonal mean atmospheric states for the warm years. These estimates correspond to the estimates of the first and second moments of the PDF for the seasonal mean atmospheric states for the warm SSTs. With the assumption that this new PDF is also normally distributed, the probabilities for seasonal mean atmospheric states to be in different categories are simply the area under the PDF that falls within the previously defined boundaries for ABN categories. Anomalous probabilities are then defined as the difference from the climatological probability, which by definition is one-third.

These anomalous probabilities are calculated in two ways. We first calculated the anomalous probabilities with the estimate for the first moment of the PDF for the warm years, but without any change in the spread of the PDF, that is, by assuming that the spread of the PDFs for warm SSTs is the same as that for the climatological distribution. This scenario is equivalent to making a categorical forecast when the impact of the SST state on the spread of the seasonal means is not known and the climatological spread is assigned for all SST states. The effect of the change in the spread is next quantified by recalculating the anomalous probabilities but with the spread estimated for the warm SST conditions. For the sake of brevity only the anomalous probabilities for the above-normal category are shown.

The anomalous probabilities for the above-normal category for the composite warm SST condition, but with the climatological spread, are shown in Fig. 8. These can be compared with the corresponding probabilities in the observations shown in Fig. 2c. As expected, the spatial patterns of the anomalous probabilities of the above-normal category look similar to the corresponding linear regressions (in Figs. 2b and 4); however, subtle differences between the two exist. For example, in the North Pacific the center of action in the anomalous probability is shifted farther to the south as compared to its location in the regression maps in Figs. 2b and 4. This is a manifestation of the fact that the anomalous probability is a function of both the shift in the PDF mean as well as its spread. Because the climatological spread tends to be smaller in the equatorward latitudes (Figs. 2a and 3), a smaller shift in the mean is as effective in producing a categorical probability anomaly as the larger shift in the mean in the northern latitudes in the presence of larger spread. This is also an explanation for the fact that the anomalous probabilities over Florida and the adjacent region are of similar magnitude as those over the North Pacific, even though the mean shift over the North Pacific is much

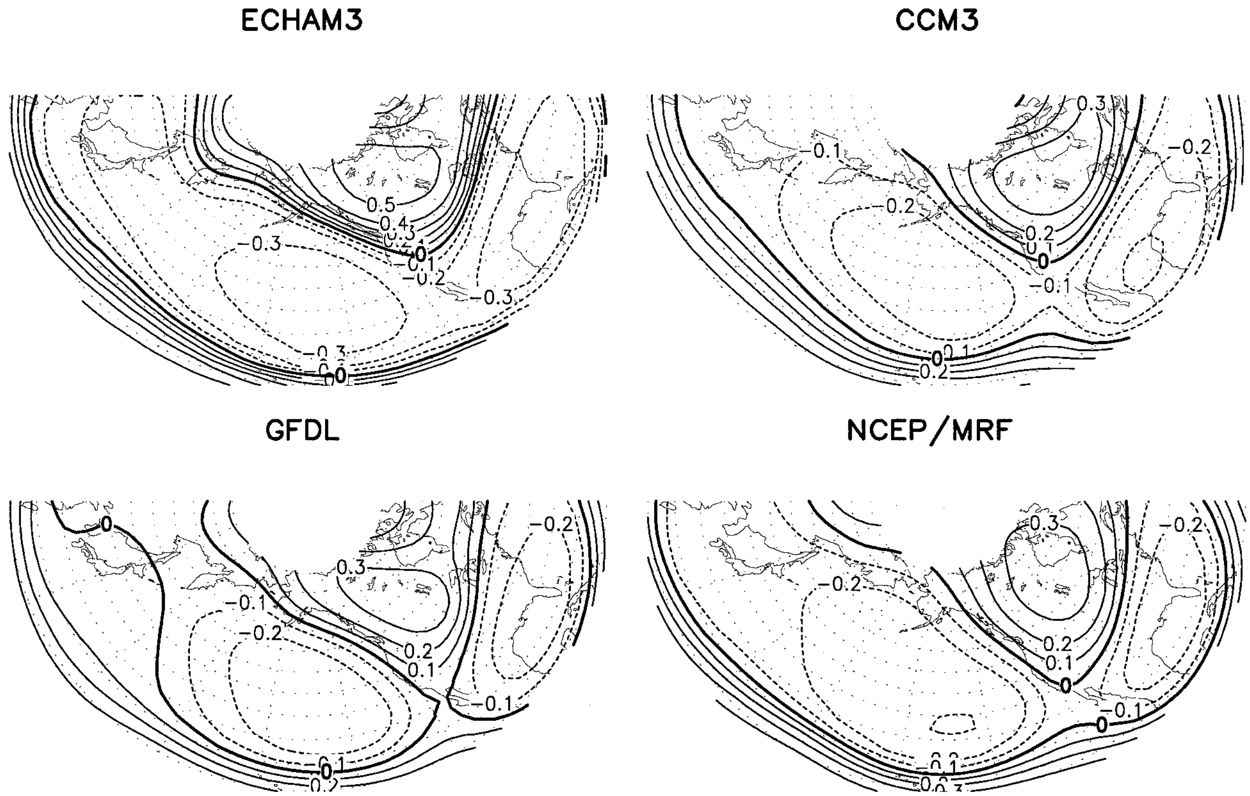

FIG. 8. AGCM-simulated anomalous probabilities for the seasonal mean 500-mb heights to be in the above-normal category for a composite warm SST event in the tropical Pacific with the assumption that the spread of the PDF for the seasonal mean height for the warm years is the same as the spread for the respective climatological PDF. Contour interval is 0.1 and negative anomalies are dashed. Positive (negative) values indicate enhanced (reduced) probability for the seasonal mean heights to be in the above-normal category. Actual probabilities for the seasonal mean heights to be in the above-normal category can be obtained by adding one-third in the anomalous probabilities.

larger than over Florida (Fig. 4). We should point out that a minimum value for the anomalous probability for the above-normal category is −0.33, while the maximum value is 0.66 (corresponding to actual probabilities of 0.00 and 1.00, respectively).

The additional contribution to the anomalous probabilities for the above-normal category when the effect of SSTs on the spread in PDF is also included is shown in Fig. 9. The contour interval in Fig. 9 is 0.025 compared with 0.1 in Fig. 8 and indicates that for each AGCM the inclusion of changes in the spread of the PDF adds little to the seasonal predictability above the existing contribution from the shift in the mean. The maximum contribution due to the inclusion of changes in the spread is for the ECHAM3 in which (over the Canadian region) the anomalous probability for the seasonal mean climate state to be in the above-normal category increases by 15%.

We should point out that in our case the spread of the climatological distribution, caused by the inclusion of all years in its definition, is always larger than the spread of seasonal mean states for warm SST conditions. This is the explanation for the fact that with the inclusion of the effect of warm SSTs on the spread, additional change in the anomalous probabilities of the above-normal category is nearly always in the same direction as the anomalous probability itself. For example, the geographical locations where the anomalous probablilites in Fig. 8 were positive (negative), the additional contribution from the impact of SSTs on the spread is also positive (negative). Exceptions are the regions in the vicinity of the zero lines in Fig. 8 where the mean of the PDF remains the same but the change in the spread will generally lead to reduced probability for seasonal mean atmospheric state to be in the above-normal category.

4. Discussion and conclusions

The focus of this paper is an analysis of the extent to which interannual variability in the tropical Pacific SSTs influences the atmospheric variability (or the spread) of the seasonal time means. For if systematic influences comparable to their well-documented impact on the seasonal mean exist, these could be utilized to enhance the skill and utility of seasonal predictions. Because only a single realization for a given SST forcing exists in the observations, estimates for the spread of atmospheric seasonal means cannot be made. Instead we use ensembles of AGCM simulations. Data from four

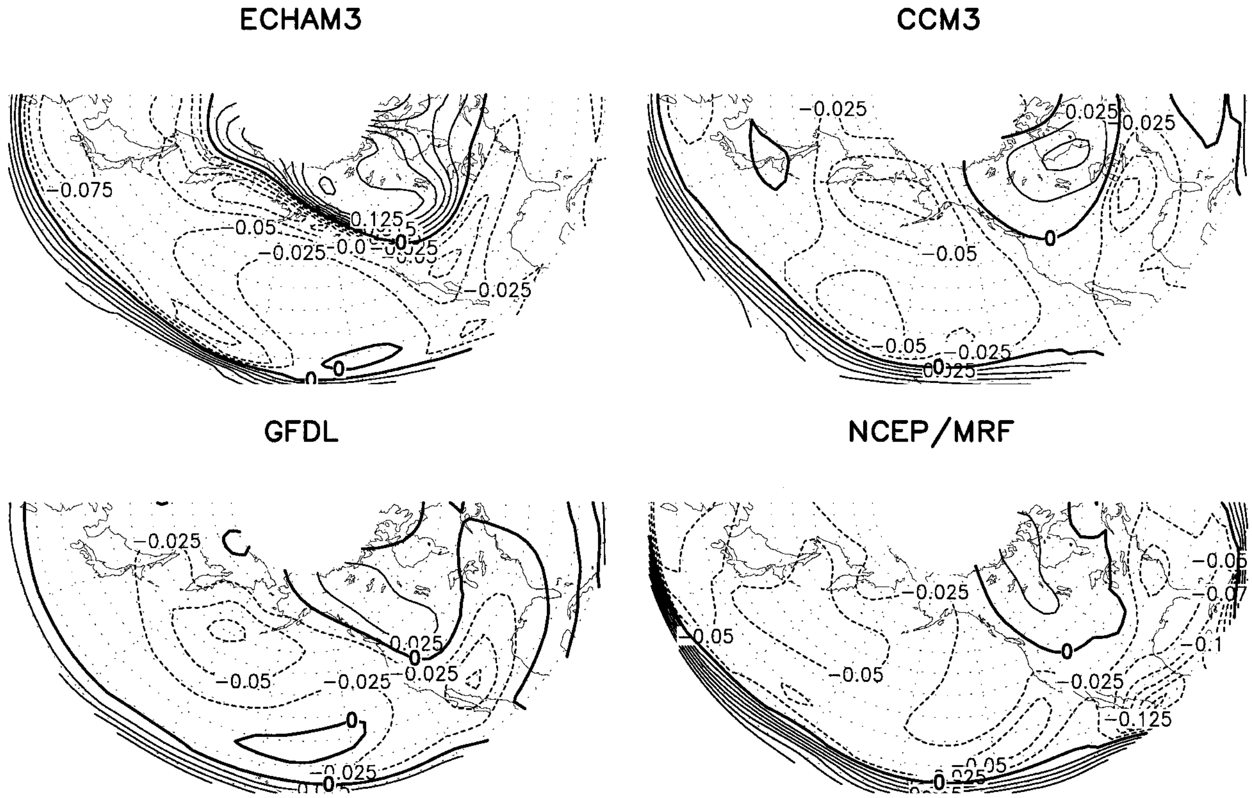

FIG. 9. Change in the anomalous probability for the seasonal mean 500-mb heights to be in the above-normal category when the effect of SSTs on the spread of the PDF is also included. This change is relative to the anomalous probabilities shown in Fig. 8. Contour interval is 0.025 and negative anomalies are dashed.

different AGCMs are utilized to ensure that results are not unduly influenced by biases in a particular AGCM.

We first compare the linear impacts of the tropical Pacific SST forcing on the mean and spread of the atmospheric seasonal time means over the PNA region. This analysis indicates that, in contrast to their well-defined impact on the time mean, the linear influence of the interannual variations in the tropical Pacific SST forcing on the spread is much weaker and has smaller spatial structures. To ensure that this is not an artifact of the linearity assumption inherent in the regression analysis, the change in the spread based on a compositing technique is also examined. This additional analysis indicates that change in the spread of the atmospheric seasonal means is larger and more systematic for warmer tropical SSTs. This finding occurs in all four AGCMs. A consistent impact of warmer SSTs is the reduction of spread over the regions south of Alaska. Similar results in the variability over these regions, but for the atmospheric flow on the subseasonal timescale, have been reported by Chen and van den Dool (1997). It is likely that reduction in the spread of seasonal means during the warm events is due to the reduction in the variability on subseasonal timescales. Further discussions about the possible physical mechanisms for the reduction in the subseasonal variability during warm events can be found in Chen and van den Dool (1997) and Palmer (1988).

Analysis of the relative contributions to seasonal predictability using a categorical forecast approach indicates a primary influence of tropical Pacific SSTs on the seasonal predictability coming from their influence on the seasonal means, with the knowledge about changes in the spread of seasonal means having little further contribution over the PNA region.

Our analysis raises the possibility that the impact of Tropical Pacific SST forcing on the spread of seasonal mean atmospheric states may be nonlinear, with larger impacts for the warmer tropical SST events. Similar (but weaker) nonlinearity in the analysis of mean response between warm versus cold events has been earlier noted by Hoerling et al. (1997). Extratropical response to the tropical Pacific SST variability is an end result of a complex chain of atmospheric processes. It remains an unresolved issue to what extent different processes in this link are most responsible for the possible nonlinear extratropical response to different phases of ENSO.

Our analysis based on categorical predictions was restricted to a composite warm (or cold) event. For larger ensemble sizes this could be easily extended to individual anomalous SST states. This in fact, is a particular advantage of the use of AGCMs for seasonal predictions, because the use of ensemble AGCM integrations allows us to construct the PDFs of seasonal atmospheric means associated with individual SST states. This advantage, however, exists when AGCMs can reproduce the atmospheric response to tropical Pacific SST conditions to sufficient accuracy.

Acknowledgments. The support offered by NOAA's Climate Dynamics and Experimental Prediction (CDEP) Program is gratefully acknowledged. GFDL model fields were provided by Issac Held, Gabriel Lau, and Mary Jo Nath as part of the GFDL-Universities Consortium Project. The CCM3 model fields were provided by Maurice Blackmon, Jim Hurrell, and Jeff Lee of NCAR's Climate and Global Dynamics Division. Thoughtful comments by two anonymous reviewers and editorial assistance of Janie Nall is gratefully acknowledged.

APPENDIX

Test of Statistical Significance of Changes in Seasonal Mean Spread during Warm and Cold Events

Because the effect of tropical Pacific SST on the spread is not strong, it is important to establish that the effect is statistically significant rather than due to chance. To address this question, a Monte Carlo test is applied. Tests can be applied to any number of aspects of the patterns shown in Figs. 6 and 7, such as the size of the locally strongest standard deviation difference, the size of this difference averaged over a defined region, or others. In our case we choose to test the standard deviation ratio rather than the difference, to normalize for the differing variances among the models (e.g., the ECHAM has the highest variance). The parameter to be tested is the sum of the absolute differences of the standard deviation ratios from unity across the entire PNA region. At each grid point the standard deviation ratio is defined as $|\sigma_w - \sigma_n|/\sigma_n$ for warm SST and $|\sigma_c - \sigma_n|/\sigma_n$ for cold SST, where σ_w, σ_c, and σ_n denote the standard deviations for warm, cold, and neutral SST years, respectively. In summing, grid points are weighted in proportion to their areal representation by multiplying by the cosine of the latitude.

With the use of a random number generator, 1000 fictitious sets of 7 warm SST years, 7 cold SST years, and 31 neutral years are generated and are subjected to the same standard deviation ratio computation, averaged over the PNA region for each model. In creating the fictitious sets of years, the years within 1950–94 period assigned as warm, cold, and neutral are randomly selected without replacement, and thus may include actual warm, cold, or neutral years to varying extents by pure chance. The idea behind the test is to determine how many of these sets of randomly categorized years result in areally integrated spread ratios as strong as, or stronger than, that which actually occurred. If very few of them do, for example, less than 50 out of 1000, then the strength of the actual pattern of ratios may be regarded as statistically significant. Because all four models produce roughly qualitatively agreeing spread difference patterns, it is suspected that these patterns may not be just by chance.

TABLE A1. Statistical significance results for effect of SST on pattern of spread of four AGCMs. Numbers in the table indicate cases out of 1000 fictitious sets of 7 warm SST years, 7 cold SST years, and 31 neutral years for which the spread exceeded that for what actually occurred for 7 warm and 7 cold events.

	IRI/ ECHAM3	NCAR/ CCM3	GFDL	NCEP/ MRF9
Warm SST	0	98	53	279
Cold SST	206	745	503	539

Results of the Monte Carlo test are shown in Table A1 for each model. Significance is achieved, or at least suggested, for the warm SST case for some of the models, while for the cold SST the results are not significant for any of the models. For the warm SST case the effects on the ECHAM model's spread are highly significant, with none of the 1000 random cases producing stronger results. The spread responses of the CCM3 and GFDL models to warm SST are suggestive, but not quite significant. The NCEP model's spread response could easily have been due to chance.

REFERENCES

Barnston, A. G., M. Chelliah, and S. B. Goldenberg, 1997: Documentation of highly ENSO-related SST region in the equatorial Pacific. *Atmos.–Ocean,* **35,** 367–383.

Blade, I., 1999: The influence of midlatitude ocean–atmosphere coupling on the low-frequency variability of a GCM. Part II: Interannual variability induced by tropical SST forcing. *J. Climate,* **12,** 21–45.

Chen, W. Y., and H. M. van den Dool, 1997: Asymmetric impact of tropical SST anomalies on atmospheric internal variability over North Pacific. *J. Atmos. Sci.,* **54,** 725–740.

Chervin, R. M., 1986: Interannual variability and seasonal climate variability. *J. Atmos. Sci.,* **43,** 233–251.

Hoerling, M. P., A. Kumar, and M. Zhong, 1997: El Niño, La Niña, and the nonlinearity of their teleconnections. *J. Climate,* **10,** 1769–1786.

Horel, J. D., and J. M. Wallace, 1981: Planetary-scale atmospheric phenomena associated with the Southern Oscillation. *Mon. Wea. Rev.,* **109,** 813–829.

Kalnay, E., and Coauthors, 1996: The NCEP/NCAR 40-Year Reanalysis Project. *Bull. Amer. Meteor. Soc.,* **77,** 437–471.

Kiehl, J. T., J. J. Hack, G. B. Bonan, B. A. Boville, D. L. Williamson, and P. J. Rasch, 1998: The National Center for Atmospheric Research Community Climate Model: CCM3. *J. Climate,* **11,** 1131–1149.

Kumar, A., and M. P. Hoerling, 1995: Prospects and limitations of seasonal atmospheric GCM predictions. *Bull. Amer. Meteor. Soc.,* **76,** 335–345.

——, and ——, 1997: Interpretation and implications of the observed inter-El Niño variability. *J. Climate,* **10,** 83–91.

——, and ——, 1998: Annual cycle of Pacific–North American seasonal predictability associated with different phases of ENSO. *J. Climate,* **11,** 3295–3308.

——, ——, M. Ji, A. Leetmaa, and P. Sardeshmukh, 1996: Assessing a GCM's suitability for making seasonal predictions. *J. Climate,* **9,** 115–129.

Lau, N.-C., 1985: Modeling the seasonal dependence of the atmospheric response to observed El Niños in 1962–76. *Mon. Wea. Rev.,* **113,** 1970–1996.

——, 1997: Interactions between global SST anomalies and midlatitude atmospheric circulation. *Bull. Amer. Meteor. Soc.,* **78,** 21–34.

Palmer, T. N., 1988: Medium and extended range predictability and stability of the Pacific/North American mode. *Quart. J. Roy. Meteor. Soc.,* **114,** 691–713.

Peng, P., A. Kumar, A. G. Barnston, and L. Goddard, 2000: Simulation skills of the SST-forced global climate variability of the NCEP-MRF9 and the Scripps–MPI ECHAM3 models. *J. Climate,* in press.

Reynolds, R. W., and T. M. Smith, 1994: Improved global sea surface temperature analysis using optimum interpolation. *J. Climate,* **7,** 929–948.

Roeckner, E., and Coauthors, 1992: Simulation of the present-day climate with ECHAM model: Impact of model physics and resolution. Max-Planck-Institut für Meteorologie Rep. 93, 171 pp. [Available from MPI für Meteorologie, Bundesstr. 55, D-20146, Hamburg, Germany.]

Rowell, D. P., 1998: Assessing potential seasonal predictability with an ensemble of multi-decadal GCM simulations. *J. Climate,* **11,** 109–120.

Smith, T. M., R. W. Reynolds, R. E. Livezey, and D. Stokes, 1996: Reconstruction of historical sea surface temperatures using empirical orthogonal functions. *J. Climate,* **9,** 1403–1420.

Trenberth, K. E., G. W. Branstrator, D. Karoly, A. Kumar, N.-C. Lau, and C. Ropelewski, 1998: Progress during TOGA in understanding and modeling global teleconnections associated with tropical sea surface temperatures. *J. Geophys. Res.,* **103** (C7), 14 291–14 324.

Zwiers, F. W., 1996: Interannual variability and predictability in an ensemble of AMIP climate simulations conducted with CCC GCM2. *Climate Dyn.,* **12,** 825–847.

——, X. L. Wang, and J. Sheng, 2000: Effects of specifying bottom boundary conditions in an ensemble of atmospheric GCM simulations. *J. Geophys. Res.,* **105,** 7295–7315.